PERSPECTIVE
https://doi.org/10.1038/s44160-022-00056-x
nature synthesis



# Reaction intermediates in the synthesis of colloidal nanocrystals

Anna Loiudice and Raffaella Buonsanti ✉

**Over the past 40 years, scientists have developed routes to synthesize colloidal nanocrystals of different compositions and with tunable size and shape. These features dictate the properties of these nanomaterials and, thus, their control aids the discovery of different physical chemical phenomena, many of which have contributed to technological advances; for example, the use of semiconductor nanocrystals as active components in displays with excellent colour purity. Yet, the synthesis of colloidal nanocrystals still proceeds by trial and error. The search for the reaction conditions to obtain nanocrystals with the desired compositions, sizes and shapes is time consuming and can fail to deliver the target product. In this Perspective, we discuss the importance of identifying reaction intermediates during the formation of colloidal nanocrystals for the development of a retrosynthetic approach to these nanomaterials. We select molecular complexes and clusters, coordination polymers and mesophases, and inorganic nanoparticles as some of the most common intermediates. The discovered pathways pinpoint the steps that enable a more predictive synthesis of colloidal nanocrystals. This Perspective encourages more mechanistic studies to eventually implement the concept of retrosynthesis for these nanomaterials.**

Colloidal nanocrystals consist of a shell of ligands around an inorganic core. The shell of ligands confers the nanocrystals with solubility in a large range of solvents and, thus, enables the formation of processable inks of semiconductors, metals and metal oxides. Quantum dots are one of the most notable examples of colloidal semiconductor nanocrystals[1,2]. Their tunable optical properties depend on both the size and shape of the nanocrystals, which makes them ideal candidates for applications such as displays and lighting devices[1,2]. Presently, quantum dots feature in high-end products of several manufacturers, such as Samsung. These semiconductor materials are also active components in mid-infrared and near infrared detectors, third-generation solar cells and brain-imaging techniques[1,2].

Metal nanocrystals have been used since the fourth century AD because of their unique optical properties[3,4]. The Lycurgus cup is one of the earliest examples of nanotechnology; this cup contains gold and silver nanoparticles that induce a colour change from green to red under illumination. More generally, the size and shape of metal nanocrystals define their optical and catalytic properties[3–6]. Indeed, the nanocrystals can tune the frequency of the surface plasmon resonance absorption and the selectivity in heterogeneous reactions[3–6]. As a consequence of these optical properties, metal nanocrystals are used in sensors for the detection of small molecules and proteins[4]. In addition, their catalytic properties have led to the commercialization of colloidal metal catalysts in industrial settings[7].

Metal oxide nanocrystals possess diverse properties, which make them appealing for various applications. Titanium dioxide and zinc oxide are largely exploited as ultraviolet light absorbers in photocatalysis and in many consumer products, which include paints and sunscreen lotions[8]. Magnetic particles, such as iron and cobalt oxides, were explored for biomedical applications as well as memory devices[9]. In recent years, multinary oxides are emerging as the active components in smart windows and in photocatalysis[2,10]. The size and shape of the metal oxide nanocrystals control the underlying properties for all these applications.

Colloidal nanomaterials are synthesized at moderate temperatures, typically below 350 °C, by the combination of metal precursors with ligands in either aqueous or organic media. The formation of nanocrystals with a certain composition, size and shape is achieved by selecting specific reaction conditions. The systematic variation of metal precursors, ligands, solvent, concentration, injection modality, reaction temperature and time enables the optimal synthesis conditions to obtain the target nanocrystals. Ligands play a key role in the size and shape control by tuning the precursor reactivity and by modulating the surface energy of the nanocrystals themselves[11].

The LaMer's model provides the classical description of the formation mechanism of colloidal nanocrystals[12–14]. This model indicates that a one-step conversion of the monomers into nanocrystals takes place (Fig. 1). The monomers are vaguely defined as the active species for nucleation. The metal precursors themselves, or other compounds that form during the synthesis, can act as the monomers. These monomers trigger nucleation when their concentration reaches the critical limiting supersaturation[12–14]. A growth stage follows this nucleation event and proceeds by the addition of the monomers to the nuclei or by attachment of the nuclei themselves[12–14]. In this classical model, a narrow size distribution may be achieved by confining the nucleation in a narrow temporal window[13,14]. The fast injection of a highly reactive precursor in a hot reaction mixture is the most common method to separate nucleation and growth to obtain monodispersed nanocrystals[13,14].

Although classical nucleation theory gives general guidelines for synthesis planning, the synthesis of colloidal nanocrystals is generally developed via a trial-and-error approach. As a huge space of experimental variables must be mapped, the optimization of the synthetic procedure for a target nanocrystal is lengthy. The desired composition, along with narrow size distribution and shape uniformity, which are all crucial parameters to control the properties, might not even be eventually obtained.

Organic chemists have the ability to target a molecule by following a retrosynthetic analysis. Retrosynthesis involves envisioning

Laboratory of Nanochemistry for Energy, Institute of Chemical Sciences and Engineering, Ecole Politechnique Fédérale de Lausanne, Sion, Switzerland.
✉e-mail: raffaella.buonsanti@epfl.ch

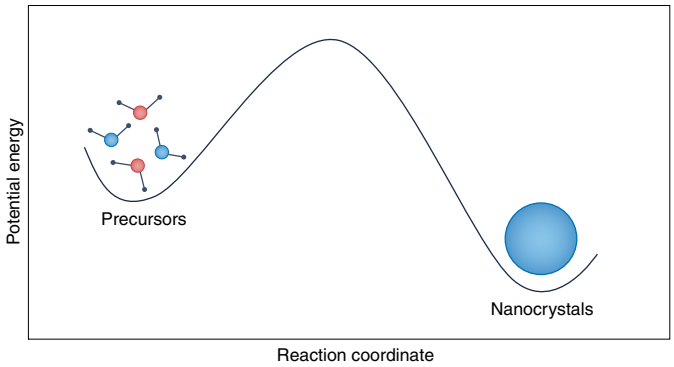


**Fig. 1 | Classical nucleation theory.** Sketch of the free-energy diagram in which a one-step conversion of molecular precursors to nanocrystals takes place according to LaMer's model.

bonds breaking in the product to form progressively simpler structures along a pathway that ultimately leads to commercially available starting materials for the synthesis. At each step, the intermediate compounds are identified. E. J. Corey, received the Nobel Prize in Chemistry in 1990 for the development of this game-changing method in the synthesis of complex molecules, following the inception of organic chemistry in the nineteenth century[15]. A dream for material chemists is to have an approach that targets materials with the desired properties in a similar way to that of organic retrosynthesis.

The chemical diversity of colloidal nanocrystals is greater than that of organic molecules. The 82 stable elements of the periodic table can be combined in the inorganic core of the nanocrystals through different type of bonds. In addition, a variety of ligands can bind to the nanocrystal surface with different configurations. Due to their intrinsic complexity, the retrosynthesis of colloidal nanocrystals cannot be envisioned as the sequential bond-breaking approach applicable to organic molecules. However, it is still possible to imagine a strategy that enables reactants and reaction conditions to be chosen a priori, with a nanocrystal with specific composition, size and shape in mind. This strategy should comprise a simplified progression of reactions, which connect isolable intermediates. To define the number of steps required, the reaction intermediates during the nanocrystal formation should be identified first. Then, these intermediates should be synthesized and developed towards the final product. To this aim, the reactions of intermediates with ligands commonly used in synthesis should be studied under a variety of conditions and the information collected in a library. This library will enable the identification of common pathways and motifs to utilize when new nanocrystals are targeted.

This Perspective showcases representative examples of mechanistic studies during the synthesis of colloidal nanocrystals. These studies use a combination of analytical techniques, which include mass spectrometry, NMR spectroscopy, in situ electron microscopy, and in situ X-ray absorption and scattering methods, to capture the complex formation pathways of nanocrystals[16,17]. Molecular complexes and clusters, coordination polymers and organic and/or inorganic mesophases and inorganic nanoparticles emerge as relatively stable intermediates across different classes of materials. The selected studies highlight how insight into these intermediates lead to a guided approach for the synthesis of target nanocrystals. This pursuit of common aspects in the synthesis of colloidal nanocrystals represents the first step towards the development of retrosynthesis and defines the theme around which our discussion is organized.

## Molecular complexes and clusters

Molecular complexes and clusters are reaction intermediates in the formation of different families of nanocrystals, which include semiconductors, metals and metal oxides. Of particular interest are anisotropic semiconductor nanocrystals, for example, wires and rods, owing to their different optical properties (such as polarized emission) compared those of spherical analogues,[1,2]. CdSe nanocrystals were among the first systems to be obtained with anisotropic shapes[18]. The synthesis of CdSe nanocrystals is typically performed in a coordinating mixture of trioctlyphosphine oxide (TOPO) and phosphonic acids[18,19]. The binding of these two ligands to specific surfaces of the CdSe nanocrystals was originally thought to drive the growth of anisotropic shapes[18]. However, a mechanistic study of their formation revealed that $(CdSe)_{17}$ clusters are key in the growth of a variety of CdSe nanocrystals[19]. These clusters possess a characteristic sharp absorption peak, which makes them distinguishable during the reaction by analysing the optical properties of aliquots taken from the reaction flask at given time intervals[19]. Experiments demonstrated that rod-shaped CdSe nanocrystals grow in the absence of the coordinating TOPO as long as $(CdSe)_{17}$ clusters form[19]. Similarly, a study showed that CdSe nanoplatelets form from small clusters via a spontaneous symmetry-breaking event followed by sequential jumps between discrete monolayer thicknesses[20].

Moving to the attractive target of heavy-metal-free quantum dots, clusters also act as reaction intermediates for the growth of anisotropic ZnSe nanostructures[21,22]. One study showed that a multistep quantized growth proceeds from nanoclusters to nanowires to nanoplatelets before it reaches the most thermodynamically stable three dimensional (3D) spherical nanocrystals (Fig. 2a)[21].

Altogether, these studies show that a successful planning of the synthesis of anisotropic semiconductor nanocrystals must aim to form clusters during the nucleation. Small clusters are stable at a high monomer concentration and, therefore, such concentrations should be targeted. In the case of CdSe, a high monomer concentration was achieved by ageing the Cd precursor solution before injecting the selenium[19]. The ageing forms a stable Cd phosphonic acid complex that slows down nucleation, generates fewer nuclei and leaves a high monomer concentration, which stabilizes the clusters[19]. The growth of the clusters should then occur under a kinetic regime. For CdSe, additional injections of the Se precursor were introduced after nucleation. The number and rate of these injections controlled the shape of the final nanocrystals. CdSe quantum rice, tadpoles, rods and branched nanocrystals were obtained with a reproducibility and uniformity that were not possible before the role of clusters as reaction intermediates was investigated and considered[19]. For ZnSe, the reaction temperature was a crucial parameter to direct the formation of different shapes (Fig. 2a)[21]. Nanowires and nanoplatelets were obtained from the same precursor at 130 and 160 °C, respectively[21].

In addition to controlling shape, the discovery of cluster intermediates has guided the synthetic approach to improve the size monodispersity of colloidal semiconductor nanocrystals, which are here exemplified by InP and CdSe quantum dots[23–26]. Previous efforts to enhance our control of the size of these nanomaterials focused on precursor reactivity[27,28]. In the case of InP, an extremely reactive phosphorus precursor, namely tris(trimethylsilyl)phosphine, was used to trigger a fast nucleation event. However, this strategy depletes the monomer reserves and, thus, prevents a growth regime that forms monodisperse quantum dots. To address this issue, the less reactive tris(triphenylsilyl)phosphine was combined in a single injection with tris(trimethylsilyl)phosphine[28]. However, the final size distribution of the InP quantum dots did not improve. This result suggests that the control of the conversion rate of the precursor into nanocrystals is not sufficient to achieve size monodispersity. In other words, the precursor does not directly convert into nanocrystals. The discovery that carboxylate-functionalized $In_{37}P_{20}(O_2CR)_{51}$ clusters form as intermediates explained this deviation[23–26].

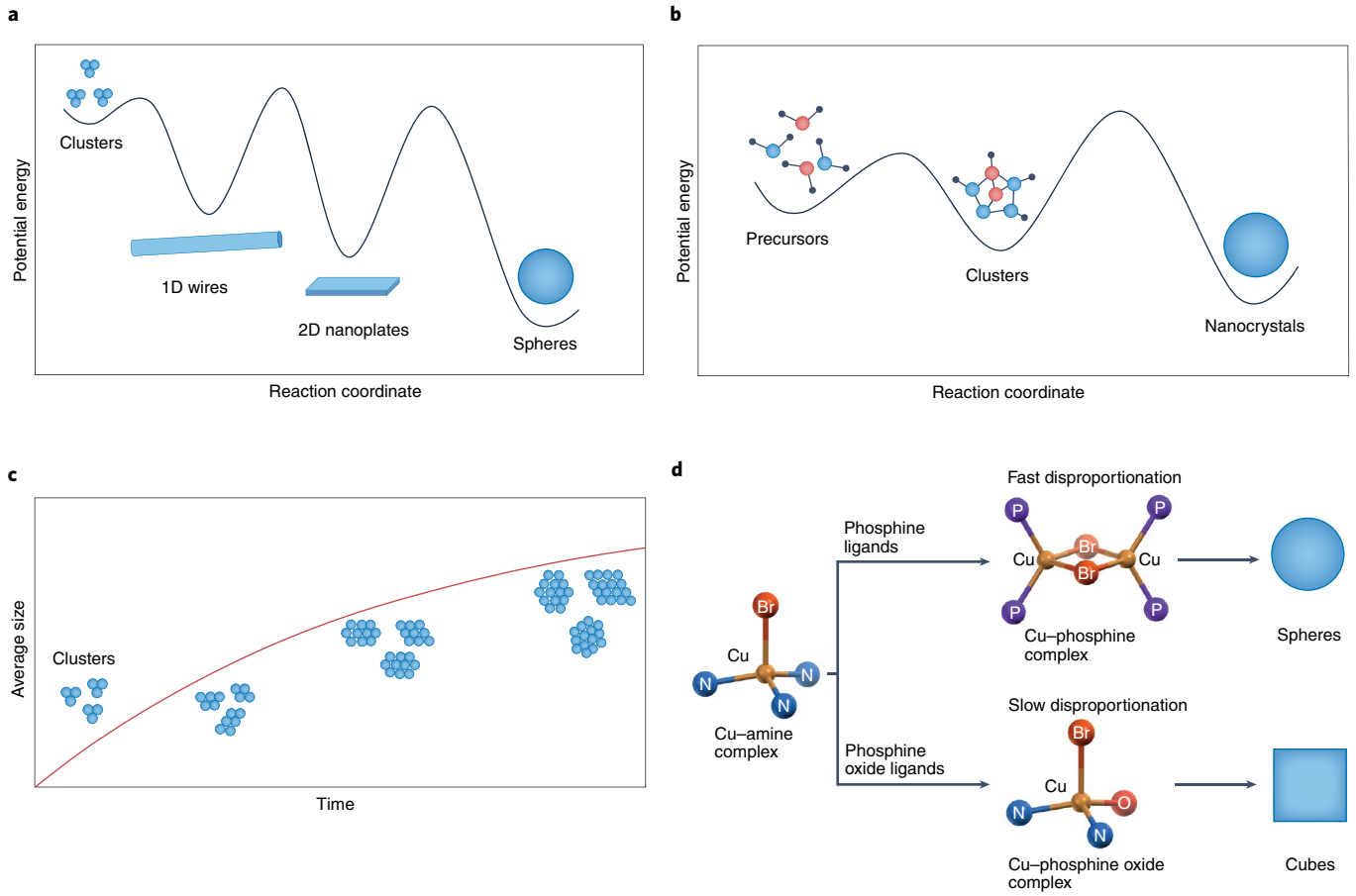


**Fig. 2 | Molecular complexes and clusters as reaction intermediates. a**, Illustration of the free-energy diagram for the formation of ZnSe nanostructures of different dimensionality. First, the molecular precursors convert into clusters, which then evolve into 1D, 2D or 3D structures through discrete steps. **b**, Sketch of the free-energy diagram for the two-step mechanism discovered for the growth of InP nanocrystals. Here, the molecular precursors convert into the $In_{37}P_{20}(O_2CR)_{51}$ clusters, which then decompose to form the nanocrystals. This discovery was crucial to narrow the size distribution of these nanomaterials. **c**, Schematic of the reaction mechanism of the continuous growth of iron oxide nanocrystals induced by the alcoholysis of tri-oxo iron clusters. **d**, Illustration of the conversion of the metal precursor into molecular complexes by reaction with the ligands during the synthesis of Cu nanocrystals. Here, the chemical nature of the complexes and their disproportionation rate control the final shape. Panels adapted with permission from **a** ref. [21], American Chemical Society; **b**, ref. [23], American Chemical Society; **c**, ref. [30], American Chemical Society; **d**, ref. [33], American Chemical Society.

In general, clusters introduce an additional local minimum in the free -energy diagram compared with that of the one-step precursor-to-nanocrystal conversion (Fig. 2b). This knowledge shifted the focus of synthesis planning from controlling the conversion rate of the molecular precursors to controlling the conversion rate of the clusters. With this aim, one strategy to increase the cluster reactivity is to modify the ligands. In fact, high-quality InP quantum dots with a narrow size distribution were obtained using primary amines as the ligands, which destabilize the clusters[23,29]. The discovery of well-defined cluster intermediates also inspired an alternative strategy to develop quantum dots with the desired average size while maintaining a narrow size distribution. This strategy involves extending the discrete growth, which is typical of well-defined clusters, to larger sizes. The potential of this strategy was recently demonstrated for CdSe quantum dots with sizes up to 3.3 nm (ref. [26]). Surface-reaction-limited conditions were crucial for the layer-by-layer growth to proceed from well-defined clusters[26]. With this knowledge, the slow ripening of well-defined clusters with optimal ligand coverage emerged as a synthetic strategy to obtain quantum dots with narrow size distributions.

In these examples, distinct nucleation and growth events are observable. However, iron oxide nanocrystals were shown to form in a continuous process[30]. In a typical synthesis, an iron molecular precursor (for example, iron chloride, iron nitrate and iron acetylacetonate) is reacted with oleic acid in the presence of a long-chain alcohol (for example, decanol or hexadecanediol)[31]. According to a previous report, the iron monomers accumulate in the reaction flask until the supersaturation conditions required for nucleation are reached[31]. Iron–oleate clusters were identified as the reaction intermediates of this process[30,32]. In the report of the continuous process to form iron oxide nanocrystals, trinuclear-oxo iron clusters were found to enlarge over time via the esterification of the oleate ligands induced by a long-chain alcohol, which contrasts with the classical idea of nucleation and growth being two separate events (Fig. 2c)[30]. In a similar manner to sol–gel chemistry, this alcoholysis generates reactive hydroxyl groups that induce condensation into intermediate iron oxygen species (such as $Fe_3O$, $Fe_4O_2$, $Fe_5O_2$ or $Fe_6O_3$). Meanwhile, the carboxylate ligands remain strongly bound to the surface of the growing clusters, and thus assure a steady-state growth to form iron oxide nanocrystals. This mechanism implies that the reaction kinetics are controlled by the rate of the alcoholysis. This discovery generated a more rational approach to synthesis planning to change the size of iron oxide nanocrystals. Indeed, shorter-chain carboxylate ligands and higher temperatures were selected to generate larger nanocrystals than those initially obtained, as these parameters increase

the rate of alcoholysis and, thus, accelerate the formation of the nanocrystals[30].

One study of Cu nanocrystals highlighted that the precursor chemistry itself provides a way to modulate the reaction kinetics and to control the shape of the nanocrystals[33]. The shape of nanocrystals typically drives selectivity in many catalytic reactions, but the tunability of the shape of Cu and other non-noble metal nanocrystals remains limited[34]. For noble metal nanocrystals, whose synthesis is generally carried out in water, there is a huge variety of accessible shapes[35], but this environment is not suitable for non-noble metals because they oxidize in water. Therefore, their synthesis must be carried out in organic solvents, for which knowledge of their formation mechanism is scarce. Cu cubes and spheres form from the reaction of CuBr in oleylamine (OLAM) with trioctlyphosphine (TOP) and TOPO, respectively (Fig. 2d)[33]. The most trivial explanation of this result is the different binding energies of TOP and TOPO to Cu surfaces. However, in situ X-ray absorption and scattering methods revealed that the CuBr reacts with TOP and TOPO in OLAM to form $(CuBr(TOP)_2)_2$ and $CuBr(OLAM)_2(TOPO)$ complexes, respectively[33]. The disproportionation of the bimetallic $(CuBr(TOP)_2)_2$ is faster than that of the monometallic $CuBr(OLAM)_2(TOPO)$. Thus, Cu nucleated at a lower temperature in the synthesis with TOP, specifically during the heating of the reaction mixture to reach the reaction temperature. The result of nucleation at low temperatures is a low monomer flux during the growth. This low monomer flux forms a spherical particle, which is the most thermodynamically stable shape for face-centred-cubic metals. On the contrary, a higher monomer flux is generated by the disproportionation of $CuBr(OLAM)_2(TOPO)$, which occurs rapidly once the reaction temperature is reached. The cubic shape, which is less thermodynamically stable than the spherical shape, is obtained as the product of the synthesis with TOPO. The knowledge that the disproportionation rate of Cu complexes governs the nanocrystal shape informed the researchers about the strategy to pursue to obtain different shapes. This strategy involves the modulation of injection rate and temperature of presynthesized Cu complexes to target metastable shapes of Cu nanocrystals. For example, Cu tetrahedra were obtained by dropwise injection of the presynthesized $CuBr(OLAM)_2(TOPO)$ at a high temperature[33].

## Coordination polymers and mesophases

Coordination polymers and mesophases are the most challenging intermediates to identify and characterize. Coordination polymers are periodic structures assembled from metal ions and ligands, and form frameworks that extend in one, two or three dimensions. Mesophases are between the liquid state and the solid state and are sometimes referred to as the 'fourth state of matter'[36]. If coordination polymers and mesophases arrange in ordered structures, which include lamellae, these intermediates can be detected by small-angle X-ray diffraction[37–42]. Amorphous mesophases, which include spinodal structures or amorphous organic–inorganic precipitates, were observed via liquid-phase electron microscopy techniques[43,44].

Several studies indicate that coordination polymers and mesophases act as 'monomer reservoirs' during the formation of nanocrystals[37–39]. In one example, at high concentrations of precursors, the formation of oleate-stabilized CdS clusters is promoted and these clusters subsequently assemble into fibrous hexagonal mesophases[37]. Then, if either the reaction time or the temperature is increased, CdS nanocrystals nucleate and grow via disassembly of the mesophase and dissolution of the clusters[37]. In a second example, in situ X-ray diffraction, scattering and absorption showed that lamellae of the coordination polymers are the intermediate in the formation of spherical Cu nanocrystals[38]. In this study, the Cu molecular precursor, which is copper acetate, reacts with the tetradecylphosphonic acid to generate layered Cu phosphonate chains (Fig. 3a). Then, trioctlyamine, which is also a reagent, reduces the Cu cations in the polymer to form metallic Cu nanocrystals. This discovery suggests that the layered Cu phosphonate chains concentrate the Cu monomers above the supersaturation level of the reaction solution. Then, the trioctlyamine triggers a burst of nucleation and monodisperse nanocrystals form (Fig. 3a). The knowledge that the polymer lamellae are the intermediate and control the size monodispersity, guided the researchers towards the steps to undertake to obtain nanocrystals with different sizes. For example, larger monodispersed nanocrystals were obtained by increasing the concentration of pre-synthesized Cu phosphonates in the reaction flask[38].

In these two studies, the coordination polymers lose their ordered structure during nucleation and generate 3D spherical nanocrystals. Other studies show that coordination polymers can act as templates to direct the growth of nanocrystals into 2D shapes, which include wires, ribbons and plates[40–42,45]. For example, the dissolution of $CdCl_2$ in primary amines formed lamellar structures that contained $(CdSe)_{13}$ clusters (Fig. 2b)[40]. The clusters recrystallize in the form of CdSe nanoribbons, which are stabilized by the dense organic layer of the lamellae (Fig. 2b). This knowledge inspired the synthesis design of CdSe nanoribbons doped with Mn by introducing $MnCl_2$ together with $CdCl_2$ (ref. [46]). These Mn-doped CdSe nanoribbons exhibited unique magneto-optical effects, which are of use for spintronic devices. These effects originate from the localized magnetic ions with the charge carriers in a strong confinement regime. The importance of 2D cluster lamellae to grow 2D structures was demonstrated for CdS also. In fact, CdS nanoribbons with a uniform thickness of 1.2 nm and of tunable lengths from around 10 nm to hundreds of nanometres were synthesized from CdS cluster lamellae[45]. The CdS nanoribbons possess a very sharp and bright emission as a result of the strong confinement regime.

The discovery of the templating effect opens up new opportunities for 2D nanostructures. The fabrication of conventional inorganic 2D semiconductors is based on high-vacuum techniques[47]. Wet chemistry offers the possibility to synthesize strain-free 2D nanostructures that are dispensable as inks. 2D nanostructures are metastable and exist only in a narrow range of reaction conditions. Thus, they are difficult to synthesize and their structural parameters not easy to tune. The knowledge that organic–inorganic compounds regulate the shape of the final nanocrystals encourages more efforts towards tuning the structure of these intermediates as a synthesis strategy. For example, increasing the thermal stability of the Cu phosphonate lamellae by changing the chain length and functional groups of the phosphonic acids may enable the preparation of 2D Cu nanostructures of different shapes, sizes and thicknesses.

## Inorganic nanoparticles

Nanoparticles were identified as reaction intermediates along different pathways of nanocrystal formation, which include aggregative growth, cation exchange and solid-state reactions in solution.

In aggregative growth, nanocrystal formation occurs via the coalescence of particles, rather than the addition of monomers to nuclei, which is described by classical theories[48,49]. When coalescence occurs along a common crystallographic direction of two adjacent particles, the aggregative growth is referred to as 'oriented attachment'[49–51]. In this case, the coalescence between the particles reduces the overall energy by removing the surface-energy term associated with unsatisfied bonds. This mechanism is relevant in cases in which particles are free to move, for example, in solution, and occurs often in biomineralization[50,51].

This mechanism is exemplified in the growth of wurtzite ZnO nanorods, in which quasi-spherical ZnO nanoparticles function as the reaction intermediates[52]. The intrinsic anisotropy of the wurtzite structure favours a spontaneous self-assembly and coalescence of the nanoparticles along the *c* axis, which explains the formation of rod-shaped nanocrystals[52].

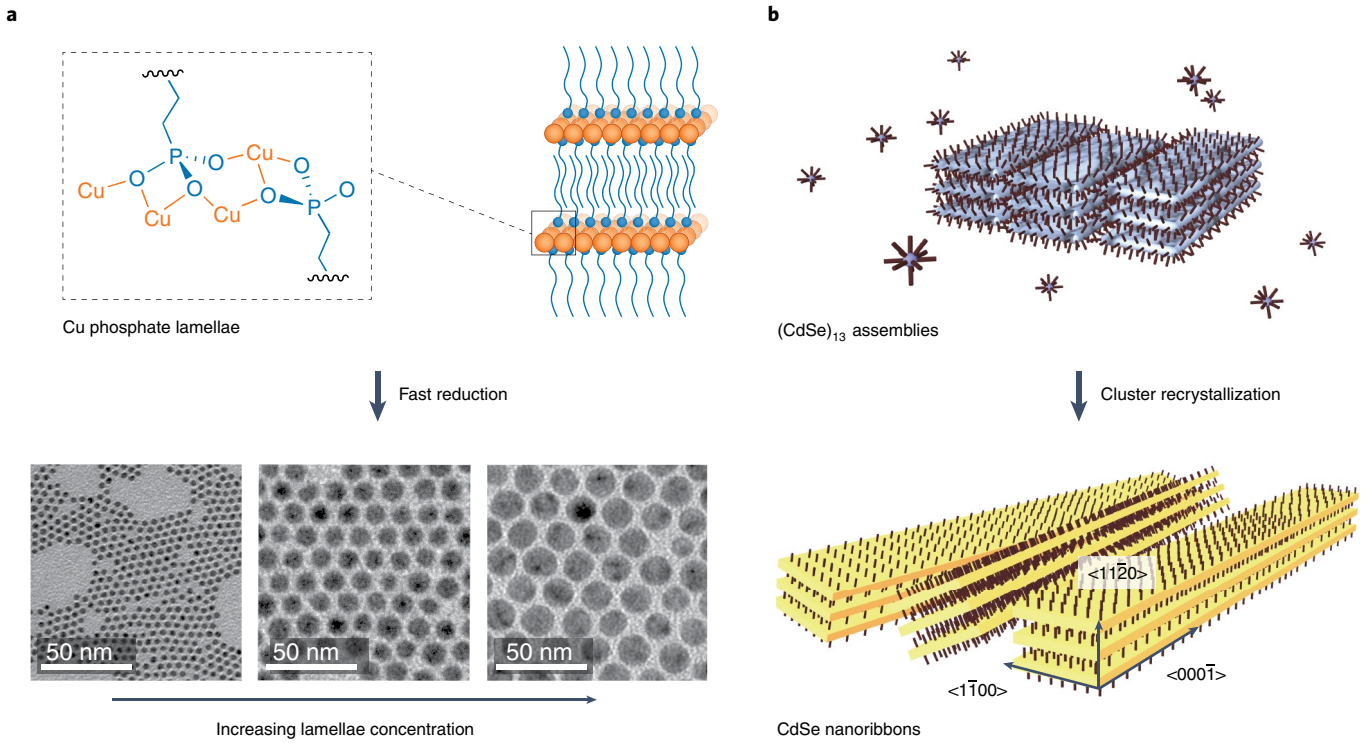


**Fig. 3 | Coordination polymers and mesophases as reaction intermediates. a**, Sketch of the Cu phosphonate coordination polymer lamellae identified during the synthesis of spherical Cu nanocrystals. The fast reduction of this intermediate by trioctylamine, which is also a reactant, causes the burst of nucleation to obtain size monodispersity. Increasing the concentration of presynthesized lamellae form spherical Cu nanocrystals with increasing size, as shown in the transmission electron microscopy images. **b**, Schematics illustrating the formation mechanism of CdSe nanoribbons. $(CdSe)_{13}$ clusters assemble into a 2D lamellar structure. CdSe nanoribbons are generated by recrystallization of the assembled $(CdSe)_{13}$ clusters. Panels adapted with permission from: **a** ref. [38], Wiley; **b**, ref. [41], American Chemical Society.

The mechanism of oriented attachment was also observed in the formation of 1D and 2D structures with a cubic crystal symmetry, such as PbS and $Pt_3Fe$ (refs. [53,54]). 2D nanosheets with lateral dimension of several hundred nanometres formed from PbS nanocrystals with a diameter of around 2–3 nm (ref. [53]). The high surface energy of the (110) surfaces on the surface of the small PbS crystallites triggers the oriented-attachment mechanism. The oleic acid molecules, which are present as ligands in the reaction mixture, densely pack on the (100) surfaces and stabilize the 2D nanosheets. In addition, it was reported that $Pt_3Fe$ nanorods form via a mechanism of oriented attachment[54]. In situ liquid transmission electron microscopy showed that nanorods form by the coalescence of small quasi-spherical particles. Initially, one nanoparticle meets another to form a dimer; then a third nanoparticle attaches to form a trimer and so on, to form a small chain of particles. Ultimately, the only observed product is long $Pt_3Fe$ chains. On the addition of oleic acid, these chains undergo a straightening reconstruction process and convert into $Pt_3Fe$ nanorods. The decrease in the total surface energy and the removal of crystal defects energetically favour the formation of the single-crystal $Pt_3Fe$ nanorods.

The knowledge that colloidal nanocrystals can form from smaller crystallites and that ligands modulate reactivity inspired the use of oriented attachment in the synthesis of nanomaterials[49]. One remarkable example is the formation of atomically coherent 2D structures from presynthesized PbSe nanocrystals[55,56]. The separation of the consecutive steps of the assembly of nanocrystals and ligand desorption was key to obtain the atomic coherence[55,56]. Indeed, atomically coherent 2D structures did not form when the assembly of PbSe nanocrystals and ligand removal from their surface occurred simultaneously[57]. In this study, first highly ordered superlattices of oleate-capped nanocrystals were formed, and then ethylene diamine was injected to selectively remove the oleic acid from (100) facets (Fig. 4a)[55]. After this deprotection step, the PbSe nanocrystals fuse with the (100) facets and form a square superlattice[55]. These nanomaterials show a high charge mobility and delocalization of the carrier over a few quantum dots, which brings the electronic properties of these 2D systems closer to those of graphene[49,55,56].

Cation exchange reactions are postsynthetic topotactic reactions that replace the cations in an ionic crystal with a new cation in the reaction medium, while keeping the anionic framework intact[58–61]. In partial exchange reactions only a fraction of the cations is replaced to produce phase-segregated heterostructured nanocrystals that contain multiple materials[58–61]. The mechanistic knowledge of the intermediates in these reactions acquired over the years is more advanced compared with that of the previously discussed cases of clusters, mesophases and oriented attachment. Indeed, in cation exchange reactions, a targeted multicomponent structure is rationally achieved by deconstructing its structure into smaller, synthetically tractable pieces. A key step in this approach is to identify easy-to-access synthons, namely, first generation (G-1) nanostructures. $Cu_{1.8}S$ spheres, rods and plates are examples of G-1 nanostructures. These $Cu_{1.8}S$ nanocrystals were transformed into second and third generation nanostructures to obtain a library of 47 derivatives via $Cu^+$ substitution with cations, such as $Cd^{2+}$, $Zn^{2+}$, $Co^{2+}$, $Ni^{2+}$ and $Mn^{2+}$. The resultant nanocrystals possessed the size, shape and uniformity of the starting material, contained up to 6 different materials, 8 internal interfaces and 11 segments (Fig. 4b)[60]. Given that all the $Cu_{1.8}S$-derived nanorods could be used as precursors, synthetic pathways towards 65,520 distinct heterostructures

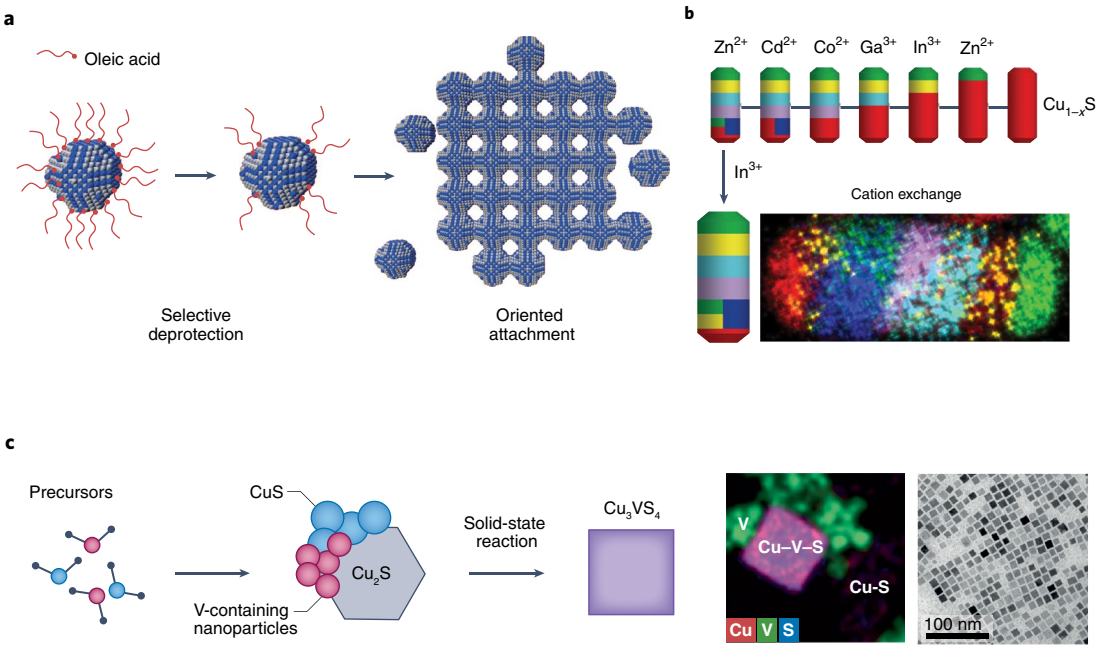


**Fig. 4 | Inorganic nanoparticles as reaction intermediates. a**, Schematic of an atomically coherent 2D superlattice made from PbSe nanocrystals. The selective deprotection of the (100) facets by the ethylene diamine triggers the oriented attachment to form the new structure. **b**, Reaction diagram illustrating the conversion of G-1 $Cu_{1.8}S$ nanorods into heterostructures that contained up to six different materials through various combinations of $Zn^{2+}$, $In^{3+}$, $Ga^{3+}$, $Co^{2+}$ and/or $Cd^{2+}$ cation-exchange steps. **c**, Illustration of the formation mechanisms of $Cu_3VS_4$ nanocrystals occurring via a solid-state reaction between $Cu_xS$ and V-containing nanoparticles (top) along with the electron microscopy analysis of the intermediates and of the final $Cu_3VS_4$ nanocubes (bottom). Panels adapted with permission from: **a**, ref. [56], Springer Nature Limited; **b**, ref. [61], AAAS; **c**, ref. [62], American Chemical Society.

were then mapped out from G-1 to the eighth generation, and 113 of these heterostructures were synthesized[61]. The interfaces and defects are not well controlled in cation exchange reactions, which compromises the material quality and related functionalities, such as optoelectronic properties. Nevertheless, this work beautifully illustrates the possibility of targeting nanomaterials in a retrosynthetic fashion. Although cation exchange reactions are applicable only to a few families of materials, which include II–VI, I–III–VI and IV–VI semiconductors, similar concepts can be translated to other compounds, such phosphides and halides.

Inorganic nanoparticles were shown to form nanocrystals in solution via solid-state reactions[62–66]. In a typical synthesis of $Cu_3VS_4$, $CuCrS_2$ and $Cu_2MnS_2$, molecular precursors of Cu and of the second transition metal were mixed together with dodecanethiol as the sulfur source[62,63]. The precursors did not directly convert into the nanocrystal products. Instead, nanoparticles of the metal sulfides and metal oxides formed and reacted during the synthesis[62,63]. Specifically, analysis of the reaction aliquots revealed that $Cu_xS$ ($x=1,2$) reacted with amorphous $VO_2$ nanoparticles to generate $Cu_3VS_4$ nanocubes with a uniform size and shape (Fig. 3c)[62]. Heterostructured nanocrystals, which included CuS and CrS nanodomains with a shared interface, were found as reaction intermediates for $CuCrS_2$ nanocrystals[63]. $Cu_2MnS_2$ formed from the solid-state reaction of $Cu_xS$ ($x=1,2$) and $MnS_y$ ($y=1,2$), which occurred in solution[63]. The balance between the metal precursor reactivity and the thiophilicity or oxophilicity of the metals explained the formation of the nanoparticles as intermediates. For example, in the case of $Cu_3VS_4$, the high oxophilicity of V and the ease of Cu–S bonding formation justifies the solid-state reaction in solution between $Cu_2S$ and $VO_2$ nanoparticles instead of the direct growth of the ternary compound from the molecular precursors.

The knowledge that ternary nanocrystals can form from nanoparticle intermediates has motivated the investigation of solid-state reactions among presynthesized nanocrystals[10,66–68]. Recent studies focused on the synthesis of multinary metal oxide nanocrystals[10]. The tunability of the composition, size and shape of these nanomaterials remains limited compared with that of other multinary compounds, for example, I–III–VI chalcogenides. Thus, new approaches to the synthesis of multinary metal oxide nanocrystals are important to understand their structure–property relationships and to exploit their potential in various applications, which include solar-driven chemistry and catalysis. The reaction between Cu and binary metal oxide nanocrystals, such as $Fe_3O_4$, $VO_2$, $Mn_3O_4$ and $GaO_x$, formed the corresponding ternary metal oxides, namely, $CuFe_2O_4$, $Cu_2V_2O_7$, $CuMn_2O_4$ and $CuGa_2O_4$[67]. Moreover, the size and shape of the products were controlled by the same features of the metal oxide nanocrystal precursors[67].

## Outlook

The synthesis of colloidal nanocrystals is still far from a retrosynthetic approach. A first step to such an approach requires deeper knowledge of the molecular chemistry of the nanomaterials and the identification of reaction intermediates, which lead to a more guided development of synthetic routes.

Next, the chemical reactions that convert the intermediates into the final products need to be understood. More specifically, reactions between the isolable intermediates and commonly used ligands should be explored to advance this knowledge. In addition, in situ characterization techniques with an improved temporal resolution will be important. In particular, X-ray absorption and scattering may answer fundamental mechanistic questions. For example, speculation remains about the mechanism of the conversion of coordination polymers and mesophases into nanostructures, which is relevant for the synthesis of 2D materials.

Along with the selection of reagents, a suitable reaction temperature profile and injection sequence of the reagents to target the desired nanocrystals are important parameters to be chosen. To tackle this challenge, an active feedback loop could be built that

correlates the chemical transformations with the changes in nanocrystal size, shape or composition during the synthesis. This idea can be more easily implemented for quantum dots, given the facile monitoring via their optical properties[69]. Heavy-metal-free semiconductor nanocrystals, such as InP and ZnSe, are interesting targets for these studies as the further development of their chemistry is likely to advance technologies based on quantum dots. Non-noble metal nanocrystals, for example, Cu, Ni and Ga and their alloys, are also worth probing because of their importance in catalysis. Monitoring the formation mechanism of these metals is more difficult compared with that of quantum dots, because non-noble metals do not have distinguishable optical features. However, their oxidation state could be monitored during the reaction via in situ X-ray absorption measurements[70].

Finally, a database of information about the reaction intermediates and formation pathways must be constructed. This database should serve as a baseline for complementing experimental data with machine-learning predictions, as has been achieved for organic synthesis[71].

Overall, retrosynthetic analysis remains a utopia in materials chemistry, where trial-and-error dominates synthetic strategies. Along with other articles focused on different materials[72,73], this Perspective encourages changes in this future direction.

Received: 4 December 2021; Accepted: 4 March 2022;
Published online: 9 May 2022

## References


1. Efros, A. L. & Brus, L. E. Nanocrystal quantum dots: from discovery to modern development. *ACS Nano* **15**, 6192–6210 (2021).
2. Kovalenko, M. V. et al. Prospects of nanoscience with nanocrystals. *ACS Nano* **9**, 1012–1057 (2015).
3. Eustis, S. & El-Sayed, M. A. Why gold nanoparticles are more precious than pretty gold: noble metal surface plasmon resonance and its enhancement of the radiative and nonradiative properties of nanocrystals of different shapes. *Chem. Soc. Rev.* **35**, 209–217 (2006).
4. Saha, K., Agasti, S. S., Kim, C., Li, X. & Rotello, V. M. Gold nanoparticles in chemical and biological sensing. *Chem. Rev.* **112**, 2739–2779 (2021).
5. Guntern, Y. T. et al. Colloidal nanocrystals as electrocatalysts with tunable activity and selectivity. *ACS Catal.* **11**, 1248–1295 (2021).
6. Cargnello, M. Colloidal nanocrystals as building blocks for well-defined heterogeneous catalysts. *Chem. Mater.* **31**, 576–596 (2019).
7. Witte, P. T. et al. BASF NanoSelect technology: innovative supported Pd- and Pt-based catalysts for selective hydrogenation reactions. *Top. Catal.* **55**, 505–511 (2012).
8. Chen, X. & Mao, S. S. Titanium dioxide nanomaterials: synthesis, properties, modifications, and applications. *Chem. Rev.* **107**, 2891–2959 (2007).
9. Wu, L., Mendoza-Garcia, A., Li, Q. & Sun, S. Organic phase syntheses of magnetic nanoparticles and their applications. *Chem. Rev.* **116**, 10473–11051 (2016).
10. Buonsanti, R., Loiudice, A. & Mantella, V. Colloidal nanocrystals as precursors and intermediates in solid state reactions for multinary oxide nanomaterials. *Acc. Chem. Res.* **54**, 754–764 (2021).
11. Heuer-Jungemann, A. et al. The role of ligands in the chemical synthesis and applications of inorganic nanoparticles. *Chem. Rev.* **119**, 4819–4880 (2019).
12. LaMer, V. K. & Dinegar, R. H. Theory, production and mechanism of formation of monodispersed hydrosols. *J. Am. Chem. Soc.* **72**, 4847–4854 (1950).
13. Kwon, S. G. & Hyeon, T. Formation mechanisms of uniform nanocrystals via hot-injection and heat-up methods. *Small* **7**, 2685–2702 (2011).
14. Lee, J., Yang, J., Kwon, S. G. & Hyeon, T. Nonclassical nucleation and growth of inorganic nanoparticles. *Nat. Rev. Mater.* **1**, 16034 (2016).
15. Nicolalaou, K. C. Organic synthesis: the art and science of replicating the molecules of living nature and creating others like them in the laboratory. *Proc. R. Soc A.* **470**, 20130690 (2014).
16. Koziej, D. Revealing complexity of nanoparticle synthesis in solution by in situ hard X-ray spectroscopy - today and beyond. *Chem. Mater.* **28**, 2478–2490 (2016).
17. Wu, S., Li, M. & Sun, Y. In situ synchrotron X-ray characterization shining light on the nucleation and growth kinetics of colloidal nanoparticles. *Angew. Chem. Int. Ed.* **131**, 9083–9091 (2019).
18. Peng, X. G. et al. Shape control of CdSe nanocrystals. *Nature* **404**, 59–61 (2000).
19. Peng, Z. A. & Peng, X. Nearly monodisperse and shape-controlled CdSe nanocrystals via alternative routes: nucleation and growth. *J. Am. Chem. Soc.* **124**, 3343–3353 (2002).
20. Riedinger, A. et al. An intrinsic growth instability in isotropic materials leads to quasi-two-dimensional nanoplatelets. *Nat. Mater.* **16**, 743–748 (2017).
21. Cunningham, P. D., Coropceanu, I., Mulloy, K., Cho, W. & Talapin, D. V. Quantized reaction pathways for solution synthesis of colloidal ZnSe nanostructures: a connection between clusters, nanowires, and two-dimensional nanoplatelets. *ACS Nano* **14**, 3847–3857 (2020).
22. Ning, J., Liu, J., Levi-Kalisman, Y., Frenkel, A. I. & Banin, U. Controlling anisotropic growth of colloidal ZnSe nanostructures. *J. Am. Chem. Soc.* **140**, 14627–14637 (2018).
23. Gary, D. C., Terban, M. W., Billinge, S. J. L. & Cossairt, B. M. Two-step nucleation and growth of InP quantum dots via magic-sized cluster intermediates. *Chem. Mater.* **27**, 1432–1441 (2015).
24. Gary, D. C. et al. Single-crystal and electronic structure of a 1.3 nm indium phosphide nanocluster. *J. Am. Chem. Soc.* **138**, 1510–1513 (2016).
25. Friedfeld, M. R., Stein, J. L. & Cossairt, B. M. Main-group-semiconductor cluster molecules as synthetic intermediates to nanostructures. *Inorg. Chem.* **56**, 8689–8697 (2017).
26. Mule, A. S. et al. Unraveling the growth mechanism of magic-sized semiconductor nanocrystals. *J. Am. Chem. Soc.* **143**, 2037–2048 (2021).
27. Harris, D. K. & Bawendi, M. G. Improved precursor chemistry for the synthesis of III–V quantum dots. *J. Am. Chem. Soc.* **134**, 20211–20213 (2012).
28. Gary, D. C., Glassy, B. A. & Cossairt, B. M. Investigation of indium phosphide quantum dot nucleation and growth utilizing triarylsilylphosphine precursors. *Chem. Mater.* **26**, 1734–1744 (2014).
29. Xie, R., Battaglia, D. & Peng, X. Colloidal InP nanocrystals as efficient emitters covering blue to near-infrared. *J. Am. Chem. Soc.* **129**, 15432–15433 (2007).
30. Chang, H. et al. Molecular-level understanding of continuous growth from iron–oxo clusters to iron oxide nanoparticles. *J. Am. Chem. Soc.* **141**, 7037–7045 (2019).
31. Kwon, S. G. et al. Kinetics of monodisperse iron oxide nanocrystal formation by 'heating-up' process. *J. Am. Chem. Soc.* **129**, 12571–12584 (2007).
32. Feld, A. et al. Chemistry of shape-controlled iron oxide nanocrystal formation. *ACS Nano* **13**, 152–162 (2019).
33. Strach, M. et al. Insights into reaction intermediates to predict synthetic pathways for shape-controlled metal nanocrystals. *J. Am. Chem. Soc.* **141**, 16312–16322 (2019).
34. Mantella, V., Castilla-Amorós, L. & Buonsanti, R. Shaping non-noble metal nanocrystals: via colloidal chemistry. *Chem. Sci.* **11**, 11394–11403 (2020).
35. Xia, Y., Xiong, Y., Lim, B. & Skrabalak, S. E. Shape-controlled synthesis of metal nanocrystals: simple chemistry meets complex physics. *Angew. Chem. Int. Ed.* **48**, 60–103 (2009).
36. Porter, R. S., Barrall, E. M. II & Johnson, J. F. Order and flow of liquid crystals. XVI. Thermodynamic order in mesophases. *Acc. Chem. Res.* **2**, 53–58 (1969).
37. Nevers, D. R. et al. Mesophase formation stabilizes high-purity magic-sized clusters. *J. Am. Chem. Soc.* **140**, 3652–3662 (2018).
38. Mantella, V. et al. Polymer lamellae as reaction intermediates in the formation of copper nanospheres as evidenced by in situ X-ray studies. *Angew. Chem. Int. Ed.* **59**, 11627–11633 (2020).
39. Gromova, M. et al. Growth mechanism and surface state of $CuInS_2$ nanocrystals synthesized with dodecanethiol. *J. Am. Chem. Soc.* **139**, 15748–15759 (2017).
40. Son, J. S. et al. Large-scale soft colloidal template synthesis of 1.4 nm thick CdSe nanosheets. *Angew. Chem. Int. Ed.* **48**, 6861–6864 (2009).
41. Yang, J., Son, J. S., Yu, J. H., Joo, J. & Hyeon, T. Advances in the colloidal synthesis of two-dimensional semiconductor nanoribbons. *Chem. Mater.* **25**, 1190–1198 (2013).
42. Liu, Y. H., Wang, F., Wang, Y., Gibbons, P. C. & Buhro, W. E. Lamellar assembly of cadmium selenide nanoclusters into quantum belts. *J. Am. Chem. Soc.* **133**, 17005–17013 (2011).
43. Loh, N. D. et al. Multistep nucleation of nanocrystals in aqueous solution. *Nat. Chem.* **9**, 77–82 (2017).
44. Yang, J. et al. Amorphous-phase-mediated crystallization of Ni nanocrystals revealed by high-resolution liquid-phase electron microscopy. *J. Am. Chem. Soc.* **141**, 763–768 (2019).
45. Son, J. S. et al. Dimension-controlled synthesis of CdS nanocrystals: from 0D quantum dots to 2D nanoplates. *Small* **8**, 2394–2402 (2012).
46. Yu, J. H. et al. Giant Zeeman splitting in nucleation-controlled doped CdSe:$Mn^{2+}$ quantum nanoribbons. *Nat. Mater.* **9**, 47–53 (2010).
47. de la Mata, M. et al. A review of MBE grown 0D, 1D and 2D quantum structures in a nanowire. *J. Mater. Chem. C* **1**, 4300–4312 (2013).
48. Wang, F., Richards, V. N., Shields, S. P. & Buhro, W. E. Kinetics and mechanisms of aggregative nanocrystal growth. *Chem. Mater.* **26**, 5–21 (2014).

49. Salzmann, B. B. V., van der Sluijs, M. M., Soligno, G. & Vanmaekelbergh, D. Oriented attachment: from natural crystal growth to a materials engineering tool. *Acc. Chem. Res.* **54**, 787–797 (2021).
50. Li, D. et al. Direction-specific interactions control crystal growth by oriented attachment. *Science* **336**, 1014–1018 (2012).
51. Penn, R. L. & Banfield, J. F. Imperfect oriented attachment: dislocation generation in defect-free nanocrystals. *Science* **281**, 969–971 (1998).
52. Pacholski, C., Kornowski, A. & Weller, H. Self-assembly of ZnO: from nanodots to nanorods. *Angew. Chem. Int. Ed.* **41**, 1188–1191 (2002).
53. Schliehe, C. et al. Ultrathin PbS sheets by two-dimensional oriented attachment. *Science* **329**, 550–553 (2010).
54. Liao, H. G., Cui, L., Whitelam, S. & Zheng, H. Real-time imaging of $Pt_3Fe$ nanorod growth in solution. *Science* **336**, 1011–1014 (2012).
55. Whitham, K. et al. Charge transport and localization in atomically coherent quantum dot solids. *Nat. Mater.* **15**, 557–563 (2016).
56. Delerue, C. Order and progress. *Nat. Mater.* **15**, 498–499 (2016).
57. Baumgardner, W. J., Withhaman, K. & Hanrath, T. Confined-but-connected quantum dot solids via controlled ligand displacement. *Nano Lett.* **13**, 3225–3231 (2013).
58. De Trizio, L. & Manna, L. Forging colloidal nanostructures via cation exchange reactions. *Chem. Rev.* **116**, 10852–10887 (2016).
59. Rivest, J. B. & Jain, P. K. Cation exchange on the nanoscale: an emerging technique for new material synthesis, device fabrication, and chemical sensing. *Chem. Soc. Rev.* **42**, 89–96 (2013).
60. Fenton, J. L., Steimle, B. C. & Schaak, R. E. Tunable intraparticle frameworks for creating complex heterostructured nanoparticle libraries. *Science* **560**, 513–517 (2018).
61. Steimle, B. C., Fenton, J. L. & Schaak, R. E. Rational construction of a scalable heterostructured nanorod megalibrary. *Science* **367**, 418–424 (2020).
62. Mantella, V. et al. Synthesis and size-dependent optical properties of intermediate band gap $Cu_3VS_4$ nanocrystals. *Chem. Mater.* **31**, 532–540 (2019).
63. Mantella, V., Varandili, S. B., Pankhurst, J. R. & Buonsanti, R. Colloidal synthesis of Cu−M−S (M = V, Cr, Mn) nanocrystals by tuning the copper precursor reactivity. *Chem. Mater.* **32**, 9780–9786 (2020).
64. Muthuswamy, E. & Brock, S. L. Solid-state phase transformations in solution: templated conversion of nanoscale nickel phosphides. *Chem. Commun.* **47**, 12334–12336 (2011).
65. Shevchenko, E. V. et al. Study of nucleation and growth in the organometallic synthesis of magnetic alloy nanocrystals: the role of nucleation rate in size control of $CoPt_3$ nanocrystals. *J. Am. Chem. Soc.* **125**, 9090–9101 (2003).
66. Schaak, R. E. et al. Metallurgy in a beaker: nanoparticle toolkit for the rapid low-temperature solution synthesis of functional multimetallic solid-state materials. *J. Am. Chem. Soc.* **127**, 3506–3515 (2005).
67. Gadiyar, C. et al. Nanocrystals as precursors in solid-state reactions for size- and shape-controlled polyelemental nanomaterials. *J. Am. Chem. Soc.* **142**, 15931–15940 (2020).
68. Lee, J. M., Kraynak, L. A. & Prieto, A. L. A directed route to colloidal nanoparticle synthesis of the copper selenophosphate $Cu_3PSe_4$. *Angew. Int. Chem. Ed.* **132**, 3062–3066 (2020).
69. Krishnadasan, S., Brown, R. J. C., deMello, A. J. & DeMello, J. C. Intelligent routes to the controlled synthesis of nanoparticles. *Lab Chip* **7**, 1434–1441 (2007).
70. Rakita, Y. et al. Active reaction control of Cu redox state based on real-time feedback from in situ synchrotron measurements. *J. Am. Chem. Soc.* **142**, 18758–18762 (2020).
71. Schwaller, P. et al. Predicting retrosynthetic pathways using transformer-based models and a hyper-graph exploration strategy. *Chem. Sci.* **11**, 3316–3325 (2020).
72. Aykol, M., Montoya, J. H. & Hummelshøj, J. Rational solid-state synthesis routes for inorganic materials. *J. Am. Chem. Soc.* **143**, 9244–9259 (2021).
73. Kovnir, K. Predictive synthesis. *Chem. Mater.* **33**, 4835–4841 (2021).


## Acknowledgements

The authors acknowledge the great support of the École Politechnique Fédérale de Lausanne over the past six years.

## Author contributions

A.L. and R.B. discussed the content and wrote the manuscript.

## Competing interests

The authors declare no competing interests.

## Additional information

**Correspondence** should be addressed to Raffaella Buonsanti.

**Peer review information** *Nature Synthesis* thanks Brian Korgel and the other, anonymous, reviewer(s) for their contribution to the peer review of this work. Primary Handling Editor: Alison Stoddart, in collaboration with the *Nature Synthesis* team.

**Reprints and permissions information** is available at www.nature.com/reprints.

**Publisher's note** Springer Nature remains neutral with regard to jurisdictional claims in published maps and institutional affiliations.